Applied Mathematics & Information Sciences
An International Journal

http://dx.doi.org/10.18576/amis/190607

Redefining Soil Stabilization Strategies: A Stochastic Exploration of Nano-Modified Clays in Foundation Engineering

Fawzi Kh. Khalaf[1,2,*], *Nur Irfah Mohd Pauzi*[1], *Mohammed Y. Fattah*[3], *Karim Sherif Mostafa*[4], *Norbaya Sidek*[5], *and Mohamed A. Hafez*[6,7]

[1] Civil Engineering Department, College of Engineering, Universiti Tenaga Nasional, Putrajaya- Malaysia
[2] Department of Building and Construction Engineering Techniques, Madenat Alelem University College, Baghdad, Iraq
[3] Faculty of Civil Engineering, University of Technology - Iraq, Al-Sina'a Street, Baghdad,10066, Iraq
[4] Civil Engineering Discipline, School of Engineering, Monash University, Malaysia
[5] Faculty of Civil Engineering, Universiti Teknologi MARA (UiTM), Selangor, Malaysia
[6] Faculty of Engineering and Quantity Surveying INTI -IU, Universi, Nilai -Malaysia
[7] Faculty of management, Shinawatra University, Pathum Thani Thailand

Received: 15 Jan. 2025, Revised: 2 Feb. 2025, Accepted: 19 Mar. 2025
Published online: 1 Nov. 2025

Abstract: This study investigates the probabilistic bearing capacity of soft clay stabilized with nanoclay, nano MgO, and nano SiO_2 using Monte Carlo Simulation (MCS). A combination of triaxial and model footing tests provided the input parameters for the stochastic analysis. MCS was applied to quantify failure probability (P_f) and reliability index (β), integrating corrected Terzaghi bearing capacity predictions through regression with experimental data. The results revealed that Nano MgO achieved the lowest P_f (4.5%) and highest β values, indicating superior strength and consistency. In contrast, Nano SiO_2, despite its high deterministic performance, showed increased uncertainty with depth, while Nano Clay exhibited poor reliability ($P_f > 59\%$). This study demonstrates that MCS provides critical insights into the variability and reliability of nano-treated soils, supporting performance-based geotechnical design under uncertainty.

Keywords: Monte Carlo Simulation (MCS), Probabilistic Geotechnics, Terzaghi Model Correction, Load–Settlement Behavior

1 Introduction

Ensuring the stability and performance of geotechnical systems under uncertain conditions remains a pressing challenge in civil engineering. Malaysia, as a developing country, is no exception; the presence of soft soil and deep strata on the western side of the Malaysian Peninsula poses significant geotechnical challenges in the construction industry. Soil properties, environmental loads, and construction processes are inherently variable, making deterministic analysis insufficient for capturing the breadth of real-world behavior. As a result, reliability-based design (RBD) has emerged as an essential paradigm for quantifying the probability of failure (P_f) and reliability index (β), thereby enabling risk-informed decision-making in geotechnical design [1, 2, 3, 4].

Among RBD techniques, Monte Carlo Simulation (MCS) is widely recognized for its versatility in handling non-linear and spatially variable systems. It enables robust probabilistic estimates, albeit often at computational expense. Studies have shown that while a few hundred to a thousand samples may suffice for second-moment statistics, up to 25,000 runs may be necessary for the accurate assessment of higher-order moments [5, 6, 7, 8]. Thus, MCS has become a benchmark method in the probabilistic evaluation of geotechnical systems, including slope stability under spatially variable conditions [9, 10, 11]. In parallel, nanomaterial-enhanced soil stabilization has sparked significant interest owing to its transformative impact on critical geotechnical

* Corresponding author e-mail: Irfah@uniten.edu.my

properties. Since Feynman's pioneering vision in 1959, nanotechnology has permeated soil mechanics, enabling enhancements in strength, stiffness, permeability, and Atterberg limits through mechanisms such as pozzolanic reactions, matrix densification, and interparticle bonding [12,13,14,15,16,17]. Nanomaterials such as nano silica (SiO_2), nano MgO, and nano clay have shown impressive improvements—up to 72% gains in unconfined compressive strength with 2% nano-MgO addition after curing [18,19,20,21]. Additionally, advances in nanocomposites, which are hybrid materials composed of two or more types of nanomaterials that exhibit synergistic properties, make them ideal for biosensing applications [40].

Despite these advancements in deterministic performance, the probabilistic implications of nanostabilization remain underinvestigated. Only limited studies—such as probabilistic assessments of nano-silica treated slopes with a P_f around 29.7% and $\beta \approx 1.64$ via machine-learning-enhanced MCS—have started to explore this gap [22,23,24,25]. The probabilistic reliability of soils treated with nano MgO and nano clay has yet to be thoroughly analyzed, leaving a critical void in current research. Integrating deterministic nanomaterial improvements with probabilistic frameworks is essential for understanding whether these performance gains hold under uncertainty and to what extent. Evaluating reliability in this context supports the prudent development of design recommendations and calibration of safety factors in practice [26] [27]. Therefore, the objective of this study is to perform a comprehensive reliability assessment using MCS on soft clay treated with three nanomaterials: nano-silica, nano-MgO, and nano-clay. This investigation will quantify (P_f and β), and the statistical distribution of bearing capacity across varying scenarios, leveraging both experimental inputs and stochastic modeling to construct a robust reliability-based design framework for nano-modified soils.

2 Material Preparation and Nanomaterial Integration Procedures

Undisturbed clay samples were collected from subsurface depths ranging between 0.5 and 1.5 meters at the Grand Al-Faw Port site in Basra, Iraq. To maintain the natural structure of the soil, auger drilling was employed during sampling, as illustrated in Figure 1. The collected specimens were subsequently oven-dried at a controlled temperature of 110(5) °C. Following drying, the soil was treated with three types of nanomaterials: nanoclay, nano-magnesium oxide (MgO), and nano-silicon dioxide (SiO_2). These materials were incorporated at concentrations between 1% and 5% of the dry weight of the soil. Each mixture underwent mechanical blending for 10 min to ensure homogeneous dispersion of the nanomaterials. The blended samples were then allowed to equilibrate for 24 h at ambient conditions before proceeding with laboratory testing.

Fig. 1: Service Quay Project Site - Grand Al-Faw Port, South of Basra, Iraq, with Soil Sampling in Progress Using Rotary Drilling Technique.

2.1 Baseline Properties of Untreated Clayey Soil

The clay soil sample underwent comprehensive physical and chemical testing to evaluate its properties for potential stabilization applications. The grain size distribution, illustrated in Figure 2 and summarized in Table 1, indicates a composition of 60% silt and 40% clay. This composition is associated with the high plasticity and expansive behavior of the soil. Based on the Atterberg limits—liquid limit (47%), plastic limit (20.5%), and plasticity index (26.5%)—the soil was classified as high-plasticity clay (CH) according to the Unified Soil Classification System (USCS) in compliance with ASTM D2487. Additionally, a shrinkage limit of 10.8% indicated moderate dimensional stability during drying.

Compaction characteristics, derived from the compaction curve in Figure 3, reveal an optimum moisture content (OMC) of 20.2% and a maximum dry density (MDD) of 15.6 $kN\,m^{-3}$, determined according to ASTM D698. These values represent the moisture content at which the soil achieves its highest compaction, which is a critical parameter for assessing its suitability for construction applications.

The chemical properties, summarized in Table 2, provide additional insights into the soil's behavior and potential challenges for structural applications. Key findings include a sulfate content of 0.94% (ASTM

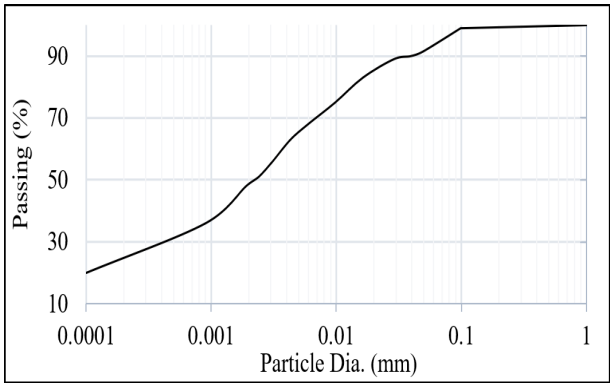

Fig. 2: Grain size distribution for the clay soil sample.

Table 1: Index Properties and Classification of Clay Soil Sample

Index Property	Index Value	Standard Specification
Specific gravity (Gs)	2.661	[28]
Silt (0.005 to 0.075 mm) (M) %	60	[29]
Clay (less than 0.005 mm) (C) %	40	[29]
Liquid limit (%)	47	[30]
Plastic limit (%)	20.5	[30]
Plasticity index (%)	26.5	–
Shrinkage limit (L.Sh.) %	10.8	[31]
Optimum Moisture Content (O.M.C) (%)	20.2	[32]
Maximum Dry Density (MDD) kN/m^3	15.6	[32]
Classification according to the (USCS)	CH	[33]

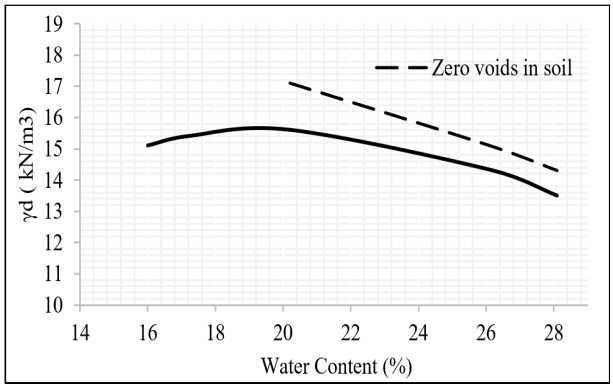

Fig. 3: Compaction curve for the clay soil sample.

D516), gypsum content of 2.72% (BS 1377-1990), total suspended solids (TSS) of 7.62% (ASTM D1888), chloride content of 2.4% (ASTM D4327), and organic matter content of 3.9% (ASTM D2974). These values are significant for evaluating potential risks, such as soil corrosion and compatibility with stabilization additives.

Table 2: Chemical Properties of Clay Soil Samples

Chemical Properties	Test Results	Standard Specification
Sulphate Content (SO_4) %	0.94	[34]
Gypsum Content (Gyp) %	2.72	[35]
Total Suspended Solids (T.S.S.) %	7.62	[36]
Chloride Content (Cl) %	2.4	[37]
Organic Matter (Org) %	3.9	[38]

3 Experimental Program Overview

To thoroughly assess the geotechnical behavior of clay soils enhanced with nanomaterials, the experimental program was structured into two main phases: (i) advanced laboratory testing using consolidated drained triaxial compression and (ii) scaled model testing of shallow foundations under controlled conditions. A total of 45 triaxial specimens were prepared to investigate the influence of nanomaterial content, ranging from 1% to 5% by dry weight, on the shear strength characteristics of the soil, particularly cohesion (c) and internal friction angle (ϕ). The nanomaterials employed in this phase include nanoclay, nano-magnesium oxide (MgO), and nano-silicon dioxide (SiO_2). The data obtained from these tests facilitated the identification of strength enhancement trends and guided the selection of the most effective dosage. Based on the observed improvements, a 3% content was deemed optimal and subsequently adopted for the model footing tests, offering a balance between mechanical enhancement, economic viability, and material efficiency.

Subsequently, 13 physical model tests were conducted using shallow foundation prototypes to simulate the bearing behavior over soils treated with the selected nanomaterials. These tests aimed to evaluate the effects of both nanomaterial type and geometry of the treated zone on the ultimate bearing capacity and load–settlement response. In addition to mechanical testing, a suite of classification tests, including Atterberg limits, compaction characteristics, specific gravity, and particle size analysis, was conducted on all treated soil samples to ensure consistency and facilitate comparative analysis.

3.1 Foundation Model for Nano-Improved Soils

Undisturbed clay samples were extracted from boreholes at the Grand Al-Faw Port site (Basra, Iraq) at depths of 0.5–1.5 m to capture key geotechnical layers. Auger drilling was employed to minimize disturbances and preserve the natural structure. The soil was oven-dried at 110(5) °C, pulverized, and characterized in accordance with ASTM standards.

Three nanomaterials were used as stabilizers:

–Montmorillonite-based Nano Clay
–Nano Magnesium Oxide (Nano-MgO)
–Nano Silicon Dioxide (Nano-SiO_2)

A fixed dosage of 3% by dry weight selected based on triaxial test performance and economic viability was thoroughly blended with designated soil portions using a mechanical mixer for 10 min, followed by a 24 hour equilibration period under ambient conditions.

3.1.1 Physical Model Configuration

A rigid steel test box (90 cm × 45 cm × 30 cm) was used to simulate the shallow foundation behavior under controlled conditions. A 4 cm × 4 cm square footing was centrally placed at the soil surface, as shown in Figure 4. Four improved geometries were tested (Table 3), each representing varying reinforcement zones beneath the footing.

Table 3: Geometric Configurations of Improved Soil Zones Beneath the Footing.

Case	Improved Zone Width (cm)	Improved Zone Depth (cm)	Geometric Representation (relative to B)
1	4	2	B × B/2
2	4	4	B × B
3	8	2	2B × B/2
4	8	4	2B × B

3.1.2 Compaction and Layering

Each test box was filled with five 5 cm layers and compacted to reach the optimum dry density (ODD) and optimum moisture content (OMC) determined from Proctor tests. The dry mass was calculated volumetrically, and the moisture content was adjusted accordingly. Each layer was compacted and leveled before the next layer was placed, with random density verification samples taken to ensure uniformity.

3.1.3 Footing Installation and Instrumentation

The model footing was placed centrally on the prepared soil surface. Dial gauges were mounted on both sides to measure settlements, with a seating load of 5 $kN\,m^{-2}$ applied for 24 h to stabilize the setup before testing, as shown in Figure 4.

3.1.4 Loading Procedure

Vertical loads were applied incrementally using a calibrated hydraulic system, as follows:

- Initial Stage: 10% of estimated ultimate capacity
- Intermediate Stage: Increased to 20% if response was linear
- Final Stage: Reverted to 10% if nonlinear behavior was observed
- Each load increment was maintained for 18 min, and settlement readings were recorded at each stage in compliance with ASTM D1194-94.

3.1.5 Failure and Data Interpretation

Failure was defined as settlement equal to 10% of the footing width (4 mm). The load corresponding to this settlement was recorded as the ultimate bearing capacity. Load–settlement curves were plotted for all test cases to assess the impact of nanomaterials on both capacity and stiffness.

3.1.6 Quality Assurance

All the procedures adhered to ASTM standards [39]. The equipment was calibrated before use, and all experiments were documented through photographs and digital logs. The selected tests were repeated to ensure reproducibility and data integrity.

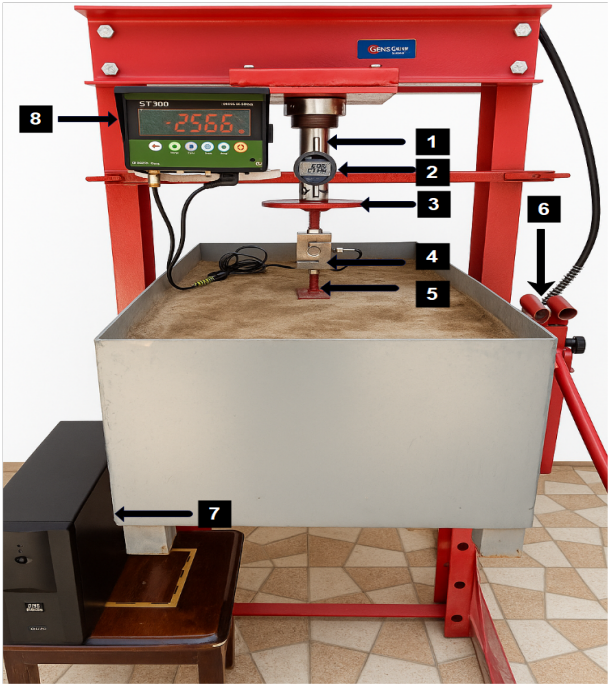

Fig. 4: Experimental Setup of Model Footing Load Test Apparatus. 1. Hydraulic Press, 2. Dial Gauge, 3. Loading Plate Connection, 4. Load Cell, 5. Model Footing, 6. Manual Jack Handle, 7. Uninterruptible Power Supply, 8. Load indicator.

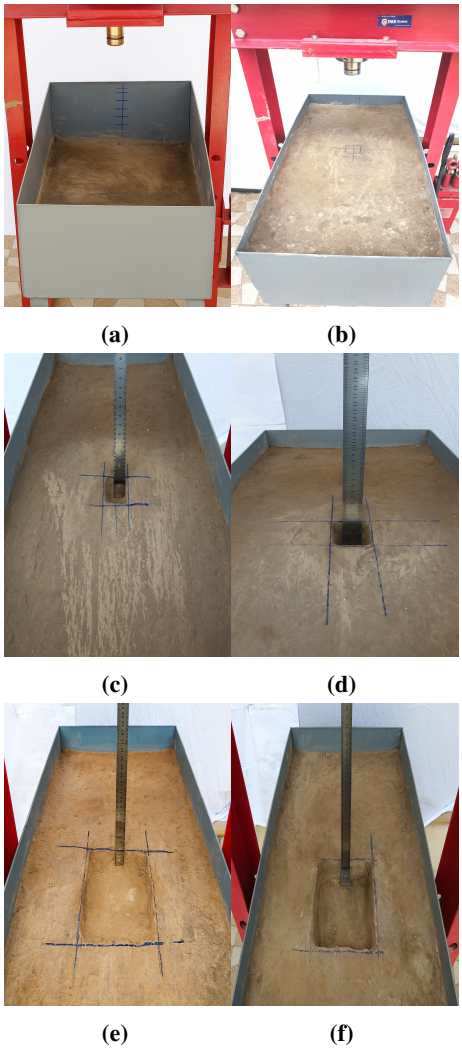

Fig. 5: A. Placing the initial soil layer and marking compaction levels. B. Leveling the compacted soil surface, C. Marking the improved zone boundaries for Case 1; D. Marking the improved zone boundaries for Case 2; E. Marking the improved zone boundaries for Case 3; F. Marking the improved zone boundaries for Case 4.

3.2 Triaxial Testing (UU Method)

To assess the short-term shear strength behavior of nano-treated clays under undrained conditions, Unconsolidated Undrained (UU) triaxial compression tests were performed in accordance with ASTM D2850-07. Specimens prepared at the optimum moisture content and maximum dry density were subjected to confining pressures of 200 kPa, 300 kPa, and 400 kPa, followed by axial loading at a constant strain rate until failure. The resulting data enabled the determination of the cohesion (c) and internal friction angle (ϕ).

Nanomaterials (nanoclay, nano MgO, and nano SiO_2) were introduced to improve interparticle bonding and structural integrity. The testing simulated rapid loading scenarios, where no drainage occurred, reflecting conditions typical of sudden load applications in the field. Uniform sample preparation was ensured by controlled tamping, dimensional checks, and membrane sealing. These findings provide critical insights into the undrained shear strength enhancement achieved through nanomodification, offering guidance for improving the immediate load-bearing performance of soft clay soils.

4 Influence of Nanomaterials on Shear Strength Parameters of Soft Clay

Table 4 illustrates that incorporating nano-silica (SiO_2) into soft clay significantly improved the soil cohesion and internal friction angle. At a 5% dosage, the cohesion value increased from 42 kPa (untreated) to 195 kPa, representing an approximate 364% improvement. The friction angle also showed significant growth, increasing from 6.3° to 10.2°. These improvements are primarily attributed to the high pozzolanic reactivity of nano-silica, which facilitates the formation of calcium silicate hydrate (C–S–H) compounds that strengthen interparticle bonds and fill voids within the soil matrix.

Additionally, the maximum dry unit weight ($\gamma_{d_{max}}$) increased to 18.5 kN m^{-3} at 4% dosage, reflecting improved soil densification. However, at 5%, a reduction to 16.8 kN m^{-3} was observed, which may indicate particle agglomeration or over-saturation, both of which reduce compaction efficiency. Overall, nano-silica demonstrated effective improvements in strength characteristics, particularly up to the 4% dosage level, making it ideal for applications requiring enhanced shear resistance and moderate stiffness.

Among all the tested nanomaterials, nano-magnesium oxide (MgO) yielded the most significant enhancement in shear strength. At 5% inclusion, the cohesion increased to 220 kPa, an improvement of over 423%, while the internal friction angle increased to 8.5°. These values indicate a strong chemical interaction between MgO and clay minerals, resulting in the formation of magnesium silicate hydrate (M–S–H) and brucite ($Mg(OH)_2$) compounds that chemically bind soil particles and improve load transfer.

Furthermore, the maximum dry unit weight reached 18.8 kN m^{-3}, the highest among all additives, while the optimum moisture content (OMC) peaked at 26.4%. These enhancements indicate an improved matrix density and water retention capacity. The linear increase in $\gamma_{d_{max}}$ with dosage suggests uniform dispersion and efficient chemical bonding throughout the soil mass. Therefore, nano-MgO presents an optimal solution for geotechnical

applications that demand high strength, stiffness, and long-term reliability.

The nanoclay exhibited moderate improvements in shear strength, primarily through physical mechanisms. The cohesion values increased from 42 kPa (untreated) to 150 kPa at 5% dosage, while the friction angle improved from 6.3° to 7.5°. These gains are largely the result of enhanced interparticle interactions, surface area effects, and void-filling capabilities rather than chemical cementation. The plate-like structure of montmorillonite in nanoclay allows for better compaction and water absorption, yet does not promote the formation of strong cementitious bonds.

The $\gamma_{d_{max}}$ improved to 18.5 kN m^{-3} at 4% dosage, but decreased slightly to 18.1 kN m^{-3} at 5%, reflecting potential limits in compaction behavior at higher dosages. The OMC increased progressively with dosage, peaking at 26.2%, indicating increased water demand for compaction. Although the performance of nanoclay does not match that of chemically reactive nanomaterials, its cost-effectiveness and environmental friendliness make it a viable alternative for projects with moderate strength requirements and less critical loading conditions.

Table 4: Influence of Nanomaterials on Shear Strength

Material	Percentage (%)	$\gamma_{d_{max}}$ (kN/m^3)	OMC (%)	Coherence (kPa)	Friction Angle(ϕ°)
Soft Clay	0	16.8	22.5	42	6.3
Nano SiO_2	1	17.6	23.8	110	7.4
Nano SiO_2	2	18.2	24.5	125	8.0
Nano SiO_2	3	18.4	25.0	140	8.7
Nano SiO_2	4	18.5	25.5	170	9.5
Nano SiO_2	5	16.8	22.5	195	10.2
Nano MgO	1	17.2	23.3	125	7.2
Nano MgO	2	17.9	24.5	150	7.6
Nano MgO	3	18.5	25.1	180	7.9
Nano MgO	4	18.7	25.5	200	8.3
Nano MgO	5	18.8	26.4	220	8.5
Nano Clay	1	16.5	22.3	52	6.5
Nano Clay	2	17.2	23.5	81	6.7
Nano Clay	3	17.9	25.1	105	7.0
Nano Clay	4	18.5	25.5	130	7.3
Nano Clay	5	18.1	26.2	150	7.5

5 Effect of Nanomaterials on q_{ult}

Table 5 shows that the incorporation of 3% nano-clay into soft clay resulted in a gradual but consistent increase in the ultimate bearing capacity across all improvement cases. Starting from 160 kPa in Case 1 and reaching 197 kPa in Case 4, the enhancement reflected a 64.2% gain over the untreated natural soil (120 kPa). This performance is largely attributed to physical stabilization mechanisms, including void filling, improved particle arrangement, and moisture retention.

Nano-clay's effects are mainly mechanical in nature, without significant chemical bonding. The limited increase in cohesion and internal friction angle suggests that the improvements are governed by enhanced compaction and better stress distribution owing to the improved soil texture. Although its bearing capacity improvement is lower than that of chemically active nanomaterials, nanoclay remains an economically viable option for light to moderate loading applications.

Among all tested materials, nano-MgO at 3% exhibited the highest improvement in ultimate bearing capacity, rising from 218 kPa (Case 1) to 275 kPa (Case 4). This corresponds to an impressive 129.2% increase compared to natural soil. The enhanced performance is directly related to chemical reactions that occur between MgO and soil constituents, leading to the formation of magnesium silicate hydrate (MSH) and brucite, which contribute to a denser, chemically bonded soil structure. The consistent trend of capacity increase across the four cases suggests high compatibility and uniform dispersion of nano-MgO in the soil matrix. Its performance confirms its suitability for critical structural applications that require a maximum load capacity and long-term stability. The results validate nano-MgO as the most efficient nano-additive for increasing the bearing strength.

Nano-silica (SiO_2) also showed a significant enhancement in bearing capacity, increasing from 196 kPa in Case 1 to 248 kPa in Case 4, equivalent to a 106.7% improvement over the untreated soil. These improvements stem from the pozzolanic activity of nano-silica, which generates calcium silicate hydrate (C-S-H) gels that strengthen interparticle bonds, reduce porosity, and improve the load-bearing framework of the soil. Compared to Nano-MgO, Nano-SiO_2 offers a slightly lower peak capacity but potentially better control over settlement owing to its finer particle size and higher surface area, which enhances soil densification. As such, nano-SiO_2 is particularly advantageous for serviceability-sensitive structures, such as pavements or lightly loaded foundations, where minimizing deformation is critical.

6 Reliability Analysis of Bearing Capacity for Nano-Treated Soils

To assess the probability of failure (P_f) and quantify the reliability of nano-treated foundation soils, a Monte Carlo simulation framework was adopted, integrating experimental data with the classical Terzaghi bearing capacity model. The workflow depicted in Figure 6, comprises the following steps:

Table 5: Mechanical performance of nano-treated soils under various foundation cases

Nanomaterial	Case	q_{ult} (kPa)
Natural Soil	All	120
Nano Clay 3%	Case 1	160
	Case 2	170
	Case 3	188
	Case 4	197
Nano MgO 3%	Case 1	218
	Case 2	240
	Case 3	255
	Case 4	275
Nano SiO_2 3%	Case 1	196
	Case 2	220
	Case 3	231
	Case 4	248

6.1 Statistical Modeling of Shear Strength Parameters

The input parameters Cohesion (c) and internal friction angle (ϕ) were obtained from UU triaxial tests and modeled as normally distributed random variables:

$$c \sim N(\mu_c, \sigma_c^2), \quad \phi \sim N(\mu_\phi, \sigma_\phi^2) \tag{1}$$

where the coefficient of variation (COV) was assumed to be 10% for both parameters, capturing moderate experimental uncertainty.

6.2 Monte Carlo Sampling and Capacity Calculation

Using $N = 10,000$ samples per case, random values of (c_i, ϕ_i) were generated and used to compute Terzaghi's bearing capacity:

$$q_{u_i} = c_i N_c + \gamma_d N_q + 0.5\gamma B N_\gamma \tag{2}$$

with bearing capacity factors calculated from ϕ using:

$$N_q = e^{\pi \tan \phi_i} \left[\tan\left(\frac{\pi}{4} + \frac{\phi_i}{2}\right)\right]^2, \tag{3}$$

$$N_c = \frac{N_q - 1}{\tan \phi_i}, \quad N_\gamma = 2(N_q + 1)\tan \phi_i \tag{4}$$

6.3 Correction Factor and Limit State Function

A regression analysis between the calculated $q_u^{Terzaghi}$ and measured q_u^{exp} values yielded a correction factor $\lambda = 0.175$ and $R^2 = 0.660$ (see Figure 13), leading to the adjusted capacity:

$$q_u^{corr} = \lambda \cdot q_u^{Terzaghi} \tag{5}$$

The limit state function is defined as:

$$G_i = q_{u_i}^{corr} - q_u^{exp} \tag{6}$$

and Failure is declared whenever $G_i < 0$, i.e., $q_{u_i} < q_u^{exp}$.

6.4 Reliability Metrics

Probability of Failure (P_f):

$$P_f = \frac{\text{count}(q_{u_i} < q_u^{exp})}{N_{sim}} \tag{7}$$

Reliability Index (β):

$$\beta = -\Phi^{-1}(P_f) \tag{8}$$

6.5 Sensitivity Analysis of Shear Strength Parameters

To further investigate the influence of input uncertainties on the bearing capacity and reliability estimates, a sensitivity analysis was conducted based on Monte Carlo simulation data. The aim was to identify which shear strength parameter cohesion (c) or friction angle (ϕ) has a greater effect on the computed bearing capacity q_u and, consequently, on the probability of failure P_f.

Using the generated sample sets of c_i and ϕ_i, the Pearson correlation coefficient between each input and the corresponding output q_{u_i} was calculated:

$$R_c = \text{corr}(c_i, q_{u_i}), \quad R_\phi = \text{corr}(\phi_i, q_{u_i}) \tag{9}$$

Results revealed that although cohesion values were numerically larger, the friction angle ϕ exhibited a strong nonlinear influence due to its exponential contribution to the bearing capacity factors N_q, N_c, and N_γ as shown in Equation (3). In particular, materials with higher ϕ (e.g., Nano SiO_2) demonstrated greater sensitivity to ϕ fluctuations. This finding underscores the importance of the accurate characterization and control of ϕ in reliability-based foundation designs involving nanomaterial treatments.

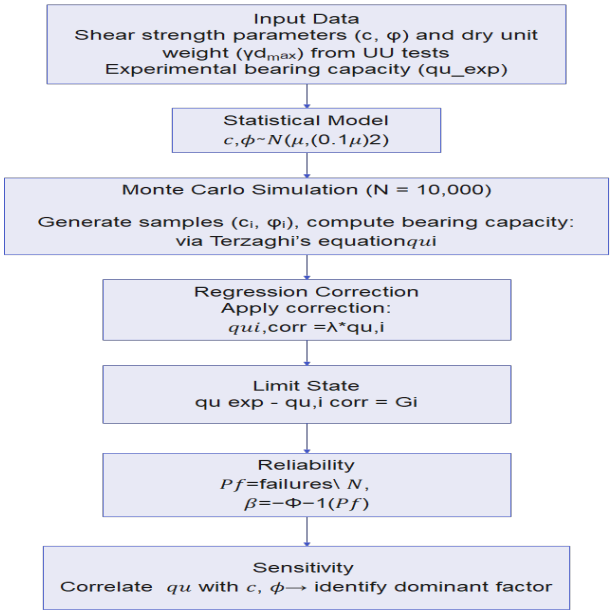

Fig. 6: Reliability Assessment of Foundations Using Monte Carlo Simulation

6.6 Stochastic Evaluation of Ultimate Bearing Capacity

The application of Monte Carlo simulation (MCS) to evaluate the ultimate bearing capacity (q_u) of nano-treated soft clay reveals valuable probabilistic insights beyond traditional deterministic analysis. For each nanomaterial, Nano Clay, Nano MgO, and Nano SiO_2—MCS generated probability density functions (PDFs) and cumulative distribution functions (CDFs) based on thousands of randomized input parameters, followed by correction using experimental data.

6.6.1 Nano Clay: High Variability and Moderate Strength Gains

The uncorrected PDF for nanoclay showed a right-skewed distribution centered around ∼1300 kPa, indicating an overestimated bearing capacity (Figure 7). The wide spread and skewness reflect substantial input variability in parameters such as cohesion and internal friction angle, combined with the relatively lower reactivity of the nanoclay.

After correction, the peak shifted to approximately 170 kPa, with a significantly narrower and symmetric distribution. The associated CDF (Figure 8) exhibited a steeper slope, indicating improved reliability and reduced uncertainty. These results highlight the necessity of calibration in probabilistic modeling—uncorrected simulations tend to produce optimistic estimates, especially for materials such as nano clay that primarily act through physical rather than chemical mechanisms.

6.6.2 Nano MgO: Highest Strength and Statistical Stability

Nano MgO demonstrated the highest bearing capacity and the most reliable probabilistic behavior. The pre-correction PDF (Figure 9) was centered around 2000 kPa, with a relatively balanced distribution, indicating robust chemical enhancement through pozzolanic reactions forming magnesium silicate hydrate (M–S–H). Post-correction (Figure 10) brought the distribution peak to ∼260 kPa, tightly clustered, and nearly symmetric, indicating both high strength and low uncertainty. The corrected CDF displayed a steep rise, showing that most values were concentrated within a narrow range, which is an ideal condition for geotechnical design. These results suggest that nano-MgO is optimal for projects requiring both high load-bearing performance and statistical predictability.

6.6.3 Nano SiO_2: Balanced Behavior with Slight Variability

Nano-SiO_2 exhibited high initial bearing capacity predictions (∼2000 kPa), similar to those of nano-MgO, as shown in its pre-correction PDF (Figure 11). However, the distribution was more right-skewed, suggesting some overestimation owing to the complex interaction between silica particles and clay minerals. The corrected distribution (Figure 12) showed a well-centered peak at ∼250 kPa with reduced spread, although slightly broader than that of Nano MgO. Its CDF confirmed moderate variability but remained within acceptable design limits. These findings position Nano SiO_2 as a balanced alternative, offering high strength and decent reliability, which is particularly valuable in applications sensitive to both bearing capacity and settlement behavior.

6.6.4 Regression Analysis: Experimental vs. Theoretical Prediction

To further support and validate the findings, a regression analysis was conducted between the theoretical Terzaghi bearing capacity values ($q^{Terzaghi}$) and the experimental bearing capacities (q^{exp}) across all nanomaterial cases. As shown in Figure 13, the regression line exhibits the following:

–Slope (λ) = 0.130

–Coefficient of determination (R^2) = 0.806

These results indicate a strong positive correlation between the classical theoretical estimations and experimental outcomes. However, the relatively low slope reflects a consistent overestimation using Terzaghi's method, particularly in soils treated with nanomaterials. This discrepancy arises because the traditional methods do not account for:

–Nano-scale chemical interactions,
–Improved microstructural bonding,
–Changes in stiffness and modulus introduced by nano-additives.

This highlights the importance of integrating empirical correction and probabilistic models to ensure safe and realistic predictions in advanced soil improvement scenarios.

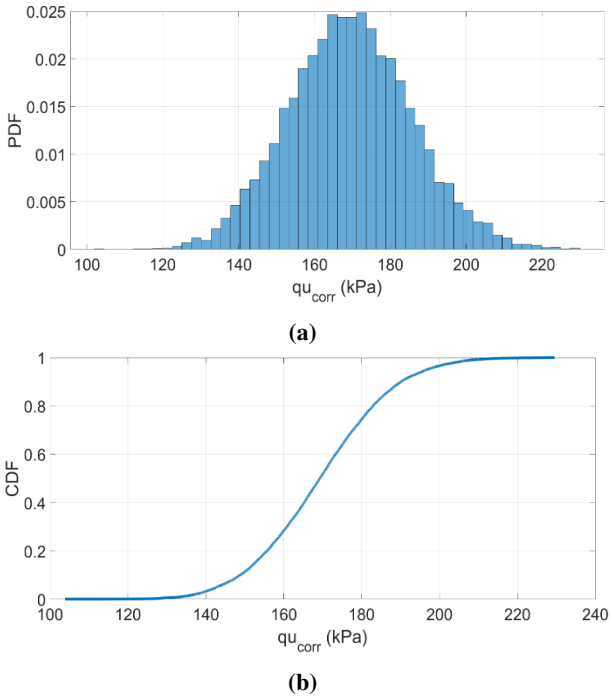

Fig. 8: Cumulative distribution function (CDF) of corrected bearing capacity for nanoclay

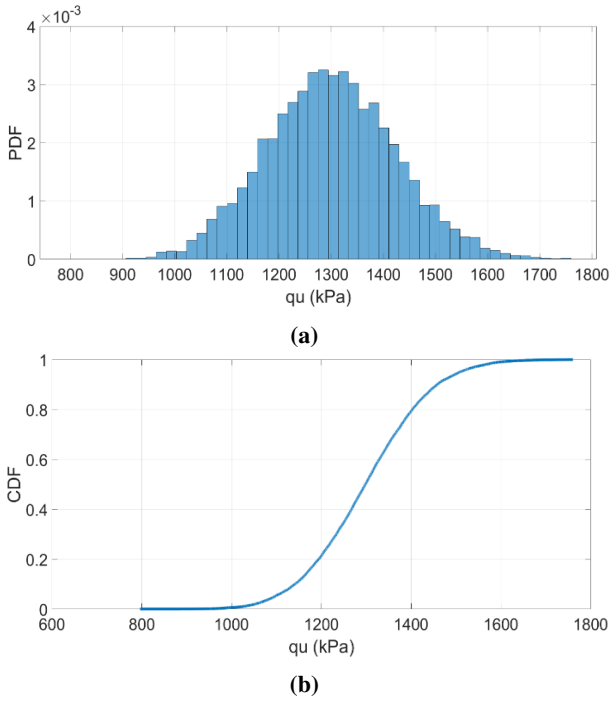

Fig. 7: Probability density function (PDF) of uncorrected bearing capacity for nanoclay

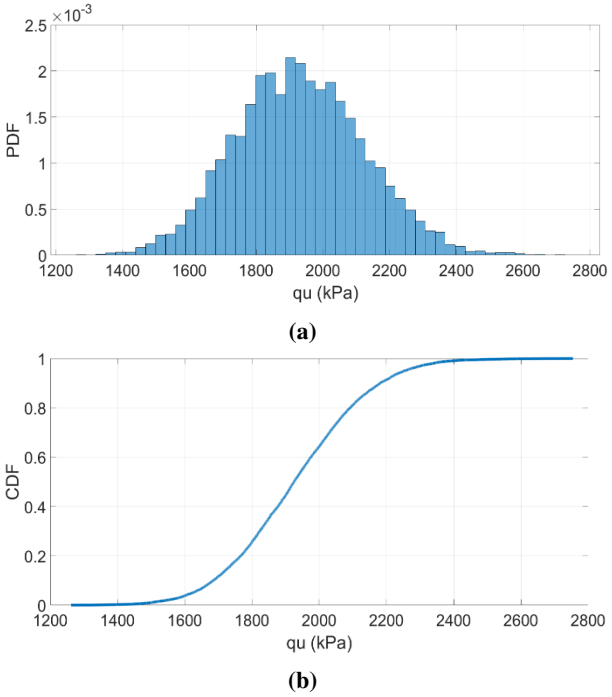

Fig. 9: PDF of uncorrected bearing capacity for Nano MgO

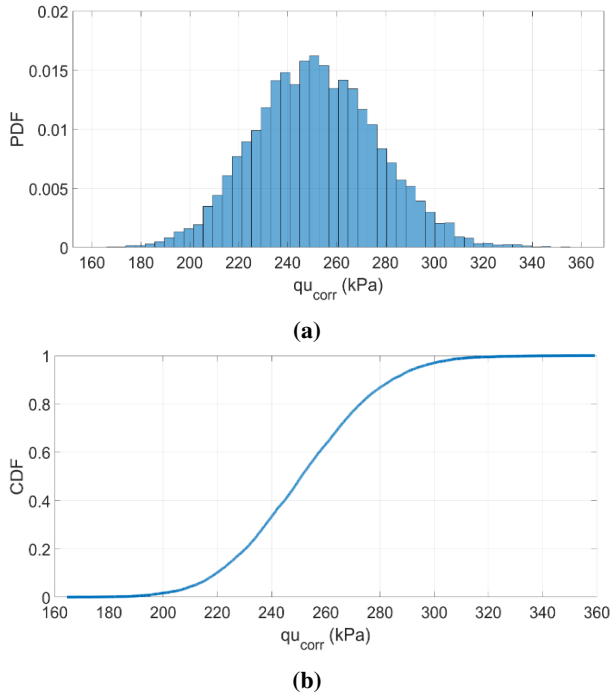

Fig. 10: PDF of corrected bearing capacity for Nano MgO

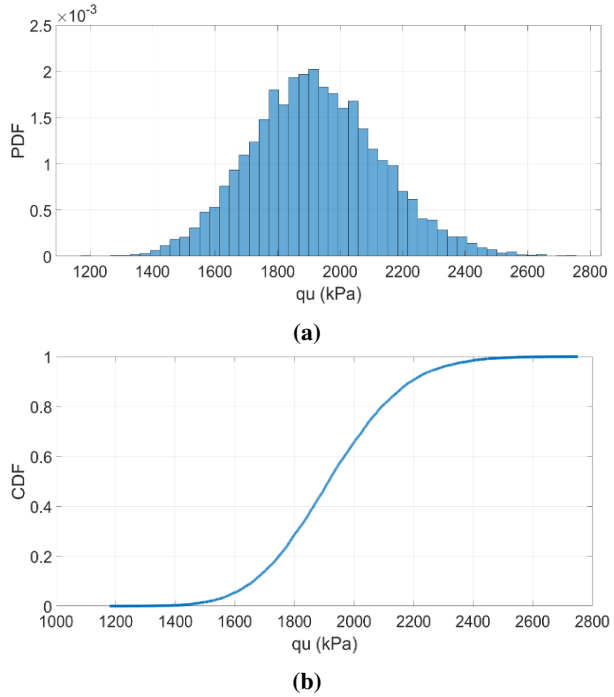

Fig. 11: PDF of uncorrected bearing capacity for Nano SiO_2

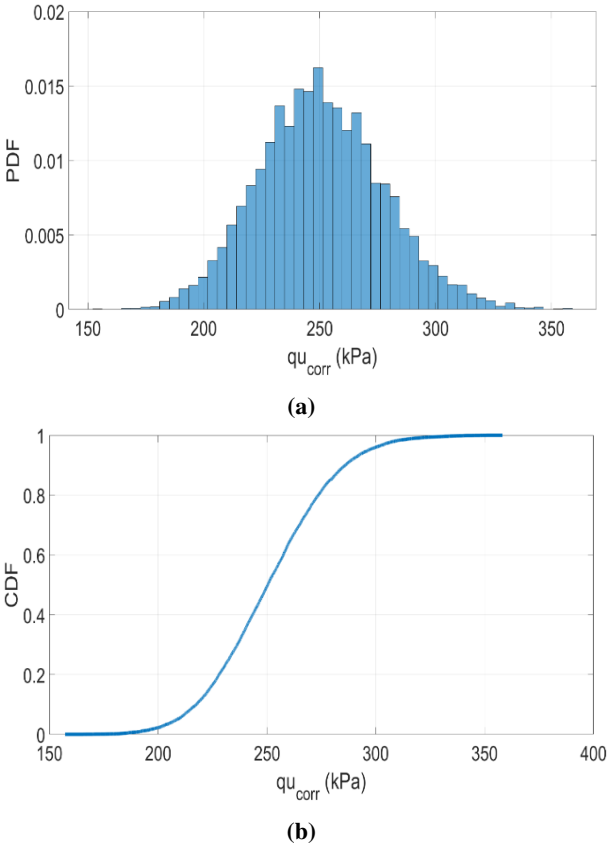

Fig. 12: PDF of corrected bearing capacity for Nano SiO_2

Combining Monte Carlo simulations, correction based on experimental data, and regression validation creates a robust, multilayered framework for analyzing and predicting the bearing capacity of nano-treated soils. Among the materials:

- Nano MgO stands out for its high strength and low uncertainty,
- Nano SiO_2 balances performance and reliability effectively,
- Nano Clay, while less powerful, still contributes to moderate improvements where cost or environmental factors are prioritized.

This study confirms that probabilistic approaches, when calibrated and validated, provide superior insights over deterministic methods alone, enabling a more informed and safer geotechnical design frameworks.

6.7 Probabilistic Sensitivity Mapping

Figure 14 presents a Monte Carlo-based probabilistic sensitivity analysis of the influence of cohesion (c) and internal friction angle (ϕ) on the ultimate bearing capacity (q_u) for three different nano-treated clay systems: Nano SiO_2, Nano MgO, and Nano Clay.

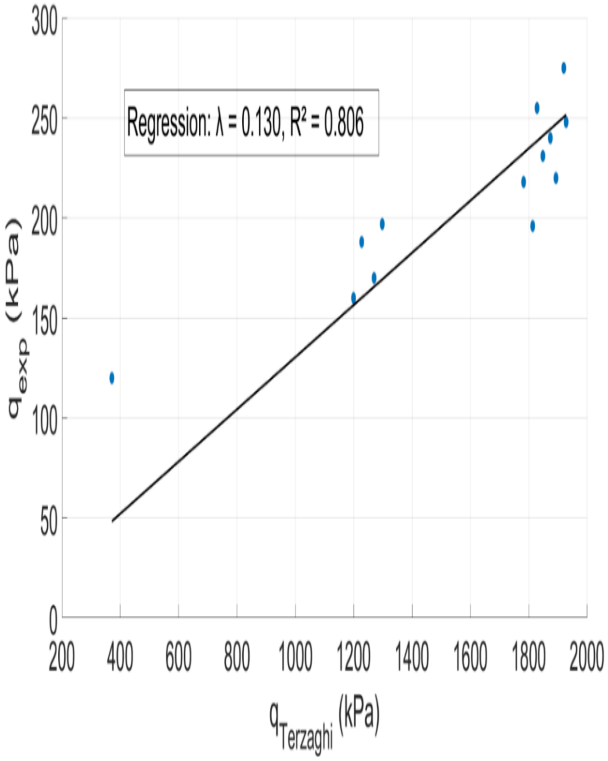

Fig. 13: Regression analysis between theoretical and experimental bearing capacities

The bearing capacity increases significantly with both the cohesion and friction angle. The color gradient (from blue to red) indicates strong sensitivity, especially at higher values of both parameters. Nano-SiO_2 exhibits a pronounced exponential sensitivity to ϕ owing to its strong pozzolanic reactions and nano-level bonding, which enhances both interparticle friction and matrix strength. Small variations in ϕ or c can result in substantial changes in q_u, indicating the need for precise control during field applications. This sensitivity also explains the relatively higher probability of failure despite the high strength gains.

The response surface is tightly clustered, suggesting high consistency in the bearing capacity with increasing c and ϕ. The distribution was dense and linear. Nano MgO-treated soils display robust mechanical behavior due to the formation of magnesium silicate hydrate (M-S-H) compounds, which chemically stabilize the soil. While sensitivity exists, it is more predictable and less variable. The uniform response confirms the statistical stability of Nano MgO, aligning with the lowest probability of failure and the highest reliability index among the nanomaterials tested.

The response surface showed a more moderate gradient with less curvature. The bearing capacity improved steadily with the cohesion and friction angle, but the rate of change was lower. This behavior reflects the physical stabilization mechanism of nanoclay, which primarily enhances the soil structure via void filling and texture improvement, rather than chemical bonding. Although the improvements are consistent, they are not dramatic. The sensitivity is moderate, indicating that nanoclay is less reactive to input variability, but also yields lower gains in bearing performance.

This analysis demonstrates how Monte Carlo simulation not only quantifies uncertainty but also maps out the interaction effects between input variables and structural performance, offering a powerful tool for probabilistic design in soil stabilization.

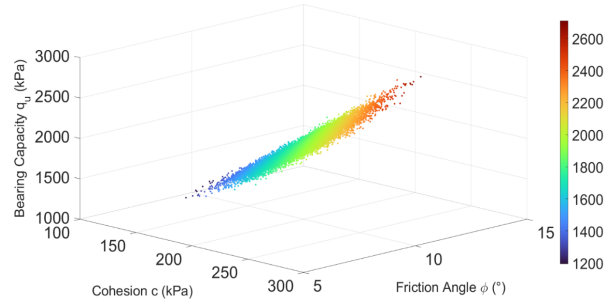

(a)

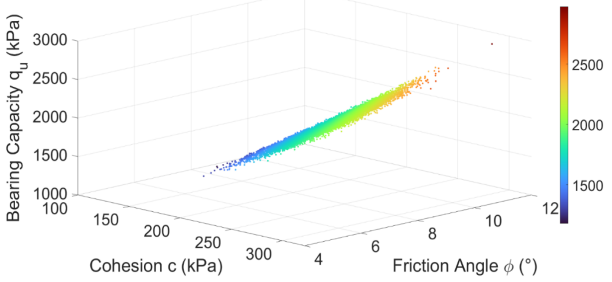

(b)

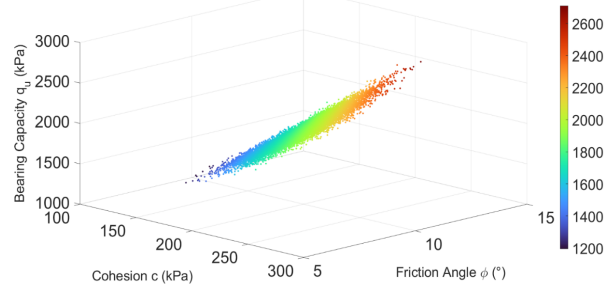

(c)

Fig. 14: 3D Probabilistic Sensitivity Mapping of Cohesion and Friction Angle on Bearing Capacity for (A) Nano SiO_2, (B) Nano MgO, (C) Nano Clay

6.8 Evaluation of Failure Probability and Reliability Index

Table 6 and Figure 15 illustrate a comparative overview of the probability of failure (P_f) and the corresponding reliability index (β) for all stabilization scenarios. As anticipated, the untreated (natural) soil exhibits a failure probability of $P_f = 1.0$, indicating a complete likelihood of failure under the considered loading conditions.

Among the treated samples, nano-MgO consistently demonstrated the most favorable reliability performance. Failure probabilities range from approximately 4.5% in Case 1 to 44.8% in Case 4, while the associated reliability indices (β) vary from +1.70 to +0.13. This trend highlights the combined effects of strength enhancement and statistical stability, likely stemming from the homogeneous dispersion of MgO particles and their controlled pozzolanic interactions with the clay minerals. The development of magnesium silicate hydrate (M–S–H) compounds plays a key role in strengthening the soil matrix and mitigating the variability in input parameters.

In contrast, nano-SiO_2, despite exhibiting high deterministic strength values, shows relatively high failure probabilities, increasing from 28.2% in Case 1 to 81.9% in Case 4. The corresponding reliability indices decline from +0.57 to –0.91, indicating reduced structural dependability with increasing treatment depth. This deterioration in reliability may be attributed to the ultrafine particle size and high pozzolanic activity of SiO_2, which may introduce greater sensitivity to changes in field conditions, such as moisture content or mixing uniformity – variables often controlled in laboratory setups but more erratic in actual site environments.

For Nano Clay, the results revealed poor reliability metrics across all test cases, with failure probabilities consistently above 59% and negative reliability indices ($\beta < 0$). This can be linked to the limited chemical reactivity of montmorillonite and its predominant physical bonding mechanism, which leads to modest improvements in shear strength. The lack of chemical binding and susceptibility to input variability significantly reduces its effectiveness in designs requiring high reliability, such as deep foundations or marine infrastructure.

6.9 Design Insights from Probabilistic Evaluation of Nano-Stabilized Soils

6.9.1 Material Selection for Reliability-Critical Applications

Among the three nanomaterials investigated, Nano MgO emerged as the most favorable additive, delivering high ultimate bearing capacities (up to 275 kPa) alongside low probabilities of failure (P_f as low as 4.5%) and high reliability indices ($\beta > 1.6$). These results underscore the consistency, chemical bonding strength via M–S–H formation, and statistical stability of nano-MgO, making it especially suitable for infrastructure projects that demand strict reliability, such as port structures, embankments, or seismic-prone zones.

In contrast, nano-SiO_2, although demonstrating significant improvements in strength and settlement behavior, revealed moderate to high failure probabilities (up to 81.9% in deeper cases) and declining reliability indices ($\beta < 0$). This suggests that while nano-silica is effective in enhancing performance, its fine particle size and high pozzolanic reactivity may lead to increased sensitivity to field variations, such as mixing quality, moisture content, and curing uniformity. Therefore, its application is better suited to serviceability-driven designs (e.g., pavements and shallow footings), where moderate failure probabilities are acceptable, but controlling deformation is critical.

Table 6: Reliability analysis results for various improvement cases

Nanomaterial	Case	Probability of Failure (Pf)	Reliability Index (β)
Natural Soil	All	1	0
Nano Clay	Case 1	0.5936	-0.2368
	Case 2	0.6154	-0.2934
	Case 3	0.9554	-1.6996
	Case 4	0.9517	-1.6616
Nano MgO	Case 1	0.0448	1.6975
	Case 2	0.1428	1.0678
	Case 3	0.3411	0.4095
	Case 4	0.4483	0.1300
Nano SiO_2	Case 1	0.2816	0.5781
	Case 2	0.4361	0.1609
	Case 3	0.7333	-0.6228
	Case 4	0.8189	-0.9112

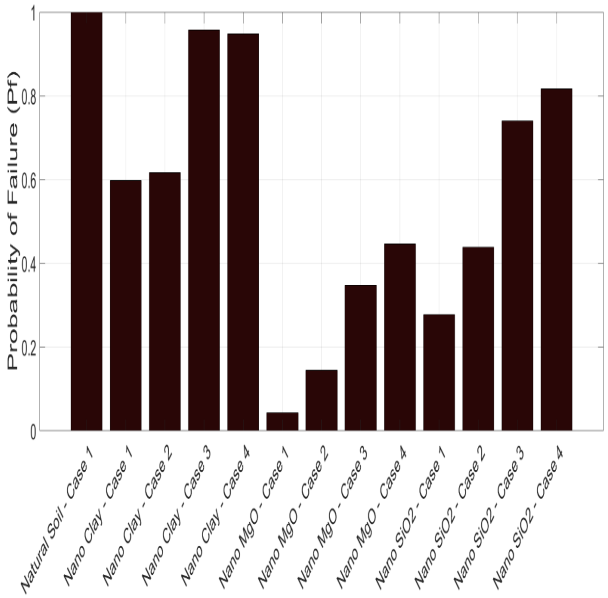

Fig. 15: Failure Probability (P_f) for All Treated and Untreated Soil Cases

Nano Clay, by comparison, showed the least favorable probabilistic performance, with all cases exhibiting $P_f > 59\%$ and $\beta < 0$. This indicates a high risk of failure under variable conditions, likely owing to its predominant physical stabilization mechanism (void-filling and texture enhancement) rather than chemical bonding. Although cost-effective and environmentally benign, its use should be limited to non-critical or temporary structures or projects with supplementary support mechanisms.

6.9.2 Influence of Improvement Geometry and Depth

The results also reveal a nuanced interaction between the geometry of the treated zone and statistical reliability. For all nanomaterials, deeper and wider improvement cases (e.g., Case 4) delivered higher deterministic bearing capacities but were more susceptible to variability, as reflected in increasing P_f values. This trend emphasizes the nonlinear relationship between treatment volume and design safety, suggesting that larger treatment zones may not always yield more reliable performance owing to scale effects, mixing heterogeneity, or moisture variation during installation. Therefore, the optimization of the improved geometry should consider not only the expected strength gain but also the resulting reliability. In high-risk scenarios, a smaller but well-controlled improvement zone may provide better overall performance than an expansive but variable one.

6.9.3 Calibration and Correction in Design Frameworks

The discrepancy between Terzaghi's theoretical bearing capacity predictions and experimental results, highlighted by a regression slope of $\lambda = 0.130$ and $R^2 = 0.806$, underscores the necessity of calibration and correction when using classical analytical models for nanomodified soils. Traditional formulas, which do not account for nanoscale interactions, microstructural changes, or modulus enhancement, tend to overestimate performance if uncorrected.

By incorporating a correction factor and utilizing Monte Carlo simulations, this study demonstrates a practical framework that can be integrated into geotechnical design codes. This approach facilitates realistic capacity estimates, supports risk quantification, and helps select safety factors based on probabilistic thresholds rather than conservative assumptions alone.

6.9.4 Towards Probabilistic Performance-Based Design (PPBD)

Ultimately, the findings advocate for a shift from traditional deterministic safety factors to performance-based design (PBD) underpinned by probabilistic tools. This methodology aligns with emerging trends in infrastructure resilience, sustainability, and cost optimization. As nanomaterials continue to evolve and become more accessible, their integration into PPBD frameworks will enable engineers to design lighter, safer, and more efficient foundations, particularly in problematic soils such as soft clays.

7 Conclusions

This research integrates experimental testing with Monte Carlo Simulation (MCS) to assess the probabilistic performance of nano-treated soft clays under shallow foundation loading. By combining the deterministic results from triaxial and model footing tests with stochastic modeling, the following conclusions were drawn:

- **Probabilistic Modeling Enhances Design Insight:** The use of MCS reveals a significant variability in bearing capacity predictions, underscoring the limitations of deterministic design alone. Calibration using experimental data is essential for realistic failure probability estimation.
- **Nano MgO Offers Superior Reliability:** Among the tested nanomaterials, Nano MgO consistently yielded the lowest probability of failure and highest reliability index (β), confirming its effectiveness in reducing design uncertainty and improving long-term performance.
- **Nano SiO_2 Requires Sensitivity Control:** Despite its high strength improvements, Nano SiO_2 showed increasing failure probabilities with treatment depth, reflecting its sensitivity to mixing uniformity and field variability. Probabilistic assessment proved vital for identifying this hidden risk.
- **Nano Clay Shows Limited Statistical Stability:** While Nano Clay improved mechanical properties moderately, it exhibited high uncertainty and failure risk across all cases, limiting its suitability for reliability-critical applications.
- **MCS as a Design Tool:** This study validates the integration of MCS into geotechnical practice as a tool for quantifying safety margins and optimizing nanomaterial selection based on both performance and probabilistic reliability.

Acknowledgement

The authors would like to thank the anonymous reviewers for their valuable comments and suggestions that helped improve the quality of this paper.

References

[1] S. M. H. Al-Riahi, N. I. M. Pauzi, M. Y. Fattah, and H. A. Abbas, "Leaching-induced alterations in the geotechnical

and microstructural attributes of clayey gypseous soils," *Ain Shams Engineering Journal*, vol. 15, no. 7, p. 102865, 2024.
[2] N. I. M. Pauzi, M. A. Aimran, M. S. Ismail, and M. S. M. Radhi, "Optimization of Egg Shell Powder and Lime for Waste Soil Improvement at Open Dumping Area Using Monte Carlo Simulations," in *Proceedings of AICCE'19: Transforming the Nation for a Sustainable Tomorrow 4*, 2020: Springer, pp. 35–46.
[3] K.-K. Phoon et al., "Geotechnical uncertainty, modeling, and decision making," *Soils and Foundations*, vol. 62, no. 5, p. 101189, 2022, doi: 10.1016/j.sandf.2022.101189.
[4] M. Porthin, L. Podofillini, and V. N. Dang, "Task reliability index for operator performance and failure probability assessment in control room simulators," *Reliability Engineering & System Safety*, vol. 251, p. 110390, 2024.
[5] O. Moselhi and M. A. Roghabadi, "Risk quantification using fuzzy-based Monte Carlo simulation," *Journal of Information Technology in Construction*, vol. 25, 2020.
[6] A. Senova, A. Tobisova, and R. Rozenberg, "New approaches to project risk assessment utilizing the Monte Carlo method," *Sustainability*, vol. 15, no. 2, p. 1006, 2023.
[7] M. A. S. Abdelmageid, "Application of Risk Management and Monte Carlo Simulation on a Construction Project (Case Study)," *Politecnico di Torino*, 2020.
[8] Y. G. Raydugin, *Modern Risk Quantification in Complex Projects: Non-linear Monte Carlo and System Dynamics Methodologies*. Oxford University Press, 2020.
[9] W. Zhang et al., "A short review of probabilistic slope stability analysis considering spatial variability of geomaterial parameters," *Innovative Infrastructure Solutions*, vol. 7, no. 4, p. 249, 2022.
[10] S. Lin, Z. Liang, H. Guo, Q. Hu, X. Cao, and H. Zheng, "Application of machine learning in early warning system of geotechnical disaster: a systematic and comprehensive review," *Artificial Intelligence Review*, vol. 58, no. 6, p. 168, 2025.
[11] C. Liu, Q. Zhang, C. Zhao, L. Deng, and Q. Fang, "Assessment of strength development of soil stabilized with cement and nano SiO_2," *Construction and Building Materials*, vol. 409, p. 133889, 2023.
[12] A. Kumar and K. Devi, "Application of Nanotechnology in Soil Stabilization," *Journal of Building Material Science*, vol. 5, no. 02, 2023.
[13] H. Mola-Abasi, M. E. Seif, H. R. Saba, and S. M. Mirhosseini, "A Bibliometric Review of the Literature on Soil Stabilization using Nanomaterials," *AUT Journal of Civil Engineering*, vol. 9, no. 1, pp. 19–32, 2025.
[14] G. Kannan and E. R. Sujatha, "Geotechnical behaviour of nano-silica stabilized organic soil," *Geomechanics and Engineering*, vol. 28, no. 3, pp. 239–253, 2022.
[15] M. Usman et al., "Nanotechnology in agriculture: Current status, challenges and future opportunities," *Science of the total environment*, vol. 721, p. 137778, 2020.
[16] A. Wahab et al., "Agriculture and environmental management through nanotechnology: Eco-friendly nanomaterial synthesis for soil-plant systems, food safety, and sustainability," *Science of the Total Environment*, p. 171862, 2024.
[17] V. Singh et al., "Chemical Constituents and Biological Activities of Cordia myxa L.: a review," *The Natural Products Journal*, vol. 12, no. 2, pp. 30–41, 2022.
[18] E. Mahmoudsaleh, A. Heidari, F. Fathi, and S. A. Hassanzadeh-Tabrizi, "Effect of nano MgO/SiO_2 additive on hydration and strength of self-compacting concrete fabricated by different processing methods," *Journal of the Australian Ceramic Society*, pp. 1–19, 2025.
[19] E. Mahmoudsaleh, A. Heidari, F. Fathi, and S. A. HassanzadehTabrizi, "Effect of Nano-MgO Additive on Compressive Strength of Concrete Fabricated by Different Processing Methods," *Journal of Advanced Materials and Processing*, vol. 10, no. 1, pp. 57–65, 2022.
[20] M. Arabani, M. M. Shalchian, and M. Payan, "A state-of-the-art review on interactive mechanisms and multi-scale impacts of nanoparticles in subgrade stabilisation," *Road Materials and Pavement Design*, pp. 1–39, 2025.
[21] N. I. M. Pauzi and T. K. Win, "Risk Assessment Prediction for Long Term Settlement using Monte Carlo Simulation for Open Dumping Area," in *MATEC Web of Conferences*, 2023, vol. 384: EDP Sciences, p. 01002.
[22] R. Fan, A. Tian, Y. Li, Y. Gu, and Z. Wei, "Research Progress on Machine Learning Prediction of Compressive Strength of Nano-Modified Concrete," *Applied Sciences*, vol. 15, no. 9, p. 4733, 2025.
[23] H. AlTawaiha, F. Alhomaidat, and T. Eljufout, "A review of the effect of nano-silica on the mechanical and durability properties of cementitious composites," *Infrastructures*, vol. 8, no. 9, p. 132, 2023.
[24] K. C. Onyelowe, A. M. Ebid, and S. Hanandeh, "The influence of nano-silica precursor on the compressive strength of mortar using advanced machine learning for sustainable buildings," *Asian Journal of Civil Engineering*, vol. 25, no. 2, pp. 1135–1148, 2024.
[25] S. M. H. Al-Riahi, N. I. M. Pauzi, M. Y. Fattah, and H. A. Abbas, "Assessment of Geotechnical Behavior of Gypseous Soil under Leaching Effect using Machine Learning," *Franklin Open*, p. 100297, 2025, doi: 10.1016/j.fraope.2025.100297.
[26] Y. Zhou, S. Zheng, and G. Zhang, "A state-of-the-art review on phase change materials integrated cooling systems for deterministic parametric analysis, stochastic uncertainty-based design, single and multi-objective optimizations with machine learning applications," *Energy and Buildings*, vol. 220, p. 110013, 2020.
[27] D. Ray and J. Ramirez-Marquez, "A framework for probabilistic model-based engineering and data synthesis," *Reliability Engineering & System Safety*, vol. 193, p. 106679, 2020.
[28] ASTM D854-14, "Standard Test Methods for Specific Gravity of Soil Solids by Water Pycnometer," ASTM International: West Conshohocken, PA, USA, 2016.
[29] ASTM D422, "Standard Test Method for Particle-Size Analysis of Soils," ASTM International: West Conshohocken, PA, USA, 2007.
[30] ASTM D4943, "Standard Test Method for Shrinkage Factors of Soils by the Wax Method," ASTM International: West Conshohocken, PA, USA, 2008.
[31] ASTM D4318, "Standard Test Methods for Liquid Limit, Plastic Limit, and Plasticity Index of Soils," ASTM International: West Conshohocken, PA, USA, 2000.
[32] ASTM D698, "Standard Test Methods for Laboratory Compaction Characteristics of Soil Using Standard Effort," ASTM International: West Conshohocken, PA, USA, 2012.

[33] ASTM D2487-17, "Standard Practice for Classification of Soils for Engineering Purposes (Unified Soil Classification System)," ASTM International: West Conshohocken, PA, USA, 2017.
[34] BS 1377, "Methods of Test for Soils for Civil Engineering Purposes," British Standards Institution: London, UK, 1990.
[35] K. H. Head, *Manual of Soil Laboratory Testing, Volume 3: Effective Stress Tests*, 2nd ed. Wiley, 1998.
[36] ASTM D5907, "Standard Test Methods for Filterable Matter (Total Dissolved Solids) and Non-Filterable Matter (Total Suspended Solids) in Water," ASTM International: West Conshohocken, PA, USA, 2018.
[37] ASTM D512, "Standard Test Methods for Chloride Ion In Water," ASTM International: West Conshohocken, PA, USA.
[38] ASTM D2974, "Standard Test Methods for Moisture, Ash, and Organic Matter of Peat and Other Organic Soils," ASTM International: West Conshohocken, PA, USA, 2007.
[39] A. W. Alshami et al., "Compaction Curves and Strength of Clayey Soil Modified with Micro and Nano Silica," *Materials*, vol. 15, no. 20, p. 7148, 2022. [Online]. Available: https://www.mdpi.com/1996-1944/15/20/7148.
[40] A. A. Shati and A. H. Alsaalamy, "Recent advances in using nanomaterials for portable biosensing platforms towards marine toxins application: Up-to-date technology and future prospects," *Microchemical Journal*, vol. 195, Dec. 2023.